Available Online

JOURNAL OF SCIENTIFIC RESEARCH

J. Sci. Res. **10**(2), 117-131 (2018)

www.banglajol.info/index.php/JSR

The Effects of Equivalence Ratio on Pressure Wave Development during Knocking Combustion

D. Deb[1*], M. A. Uddin[1], H. Terashima[2], N. Oshima[2]

[1]Department of Mathematics, Shahjalal University of Science & Technology, Sylhet, Bangladesh

[2]Division of Mechanical & Space Engineering, Hokkaido University, Hokkaido, Japan

Received 11 July 2017, accepted in final revised form 26 January 2018

Abstract

A knocking combustion in a one-dimensional constant volume reactor has been simulated with a detailed chemical kinetic mechanism of *n*-heptane premixed gases by using the compressible Navier-Stokes equations. This study focuses on the impact of the various equivalence ratios (0.6–1.4) in the pressure wave development during knocking combustion in an account of different initial temperature (600–900K). The result demonstrates the autoignition process in the end-gas region and explains the knocking phenomenon on different equivalence ratio. In an adiabatic wall condition, the largest knocking intensity occurs in equivalence ratio 1.4 whereas the lowest knocking intensity found in equivalence ratio 0.6. Regarding to initial temperatures, a strong peak of knocking is generated around 650K in all the equivalence ratios (0.8–1.4). However, yet a small perceptivity of knocking is found in around 750K for each equivalence ratio. In case of smaller equivalence ratios, a weak knocking occurs, which can be identified by the behavior of the pressure wave generation in the end-gas region.

Keywords: End-gas; Autoignition; Knocking; Equivalence ratio; *n*-heptane.

doi: http://dx.doi.org/10.3329/jsr.v10i2.34491 J. Sci. Res. **10** (2), 117-131 (2018)

1. Introduction

Knocking is one of the major phenomena of abnormal combustion to gain higher thermal efficiency in spark-assisted engines. Knocking is strongly related to the presence of pressure oscillation and has been not only a massive interruption to increase compression ratios, but also a direct constraint on engine performance [1]. Knocking combustion ascertains engine stability, fuel consumption and even noise and emission rate of poisonous gases. Enormous researches have been carried out to explain the mechanism of knocking combustion, to identify the influencing factors and to develop countermeasures against engine knock. Moreover, it is not yet to invent completely the mechanism and resistant of knocking cause the phenomenon of knocking is still complicated [2].

* *Corresponding author*: dipokdeb009@gmail.com

One of the reasons for the occurrence of knocking is the end-gas autoignition ahead of a normal flame front propagated in combustion chamber [3]. During end-gas autoignition, a pressure wave is generated and developed with a large amount of unburned mixture, which may lead to a strong pressure wave neration such as detonation [4]. An influence of nonhomogeneous temperature distribution during combustion is another reason for the formation of knock, which is observed by the experiment of Pöschl and Sattelmayer [5]. Due to such temperature inhomogeneities, a fast propagating flame is generated, and autoignition occurs in the end-gas region, which initiates a pressure vibration and knocking phenomena. However, the relationship between temperature inhomogeneities and knocking remains unclear.

For understanding knocking, we need interaction between the fluid and chemical reaction. Recently, numerical methods have been developed in fuel chemistry to know the details behavior between the fluid and chemical reaction. Computational simulation is an essential tool to realize the flow structures in the interaction between fluid dynamics and detailed chemical kinetics mechanisms for large hydrocarbon fuels with the latest high-performance computers [6]. However, the number of detailed numerical studies involving large hydrocarbon fuels for knocking combustion is unluckily restricted by this laborious work.

At first, Pitz and Westbrook [7] investigated the impermanent behavior of laminar flame propagation during autoignition of an end-gas for Propane and n-Butane by using the chemical kinetics mechanisms. They observed strong acoustic waves had been created and propagated in the burnt gases due to high heat release rates during end-gas autoignition. Sequentially, to examine the behaviors of reaction front propagation from hot or cool spots in an end–gas autoignition, detailed numerical computations have been performed [8,9]. Five modes of reaction front propagation from a hot-spot using one-dimensional (1-D) flow equations with detailed chemical kinetic mechanisms of $H_2 - CO - \text{air}$ and $H_2 - \text{air}$ mixtures have been identified by Gu *et al.* [8], which rely on the parameter, initial hot spot temperature gradient normalized by the critical temperature gradient. But their investigations also demonstrate that this dimensionless parameter is inadequate to describe properties fully the limits of developing detonation mode. Another theoretical relationship between dimensionless parameter, overpressure, and noise generated by end-gas autoignition has been discussed by Bradley and Kalghati [10] using different fuels of mixtures.

Subsequently, Ju *et al.* performed a 1-D simulation with a detailed chemical kinetic mechanism of *n*-heptane at an equivalence ratio of 0.4 without assuming temperature gradients [11]. Flame front propagation, end-gas autoignition and reaction front propagation have been numerically simulated in this study where the flame front dynamically interacted with the end-gas through the propagation. They explained the dependency of ignition delay time and transient pressure histories on a different initial temperature of *n*-heptane-air mixtures at equivalence ratio 0.4 which ensues hot ignition and may cause acoustic wave oscillations in the reactor. They did not find any reason for transient oscillatory behavior initiated by the end-gas autoignition and cannot clarify any

relationship between equivalence ratio and transient pressure wave development. As a sequential way, a transient one-dimensional reaction front simulation has been conducted by Martz *et al.* [12] under thermodynamic conditions to elucidate the process of premixed reaction front propagation during end-gas autoignition.

The detailed mechanism of pressure wave generation in end-gas autoignition during knocking combustion is clarified by Terashima and Koshi [13]. They conducted numerical simulation by using a one-dimensional constant volume reactor where two pre-mixed gases *n*-butane/air and *n*-heptane/air have been considered with an equivalence ratio 1.0. Largely detailed chemical kinetics mechanisms are being used in this simulation under the adiabatic wall and isothermal wall condition. Their study elucidated that, strong knocking phenomenon occurs in the presence of temperature inhomogeneities in the end-gas. The growth of temperature inhomogeneities is increased by the appearance of the NTC region through heat release by low-temperature oxidation. Thus, a strong pressure wave generated at the wall and in the region ahead of the flame front and propagated in the whole reactor due to inhomogeneous autoignition in the end-gas. However, they did not address any effect of equivalence ratio on pressure wave development during knocking combustion.

For the development of SI Engine, one of the major challenges is to suppress knocking. We need lean-combustion for efficient fuel use to suppress the knock. But there is a lacking, at a different equivalence ratio, the mechanism of pressure and temperature changes in end-gas autoignition during knocking combustion. In this study, we consider fuel chemistry in the coupling of the compressible Navier-Stokes equation with a detailed chemical kinetic mechanism for premixed gas *n*-heptane/air. The objective of this numerical study is to investigate the effects of equivalence ratio on pressure wave development in the end-gas during knocking combustion.

2. Computational Method

2.1. *Governing equations and model*

In the present study, the flow fields are modeled with the compressible Navier-Stokes equations and the thermally perfect gas equation of state, which is given as follows:

$$\frac{\partial \rho}{\partial t} + \nabla.(\rho \boldsymbol{u}) = 0 \tag{1}$$

$$\frac{\partial (\rho \boldsymbol{u})}{\partial t} + \nabla.(\rho \boldsymbol{u} \otimes \boldsymbol{u} + P\delta - \boldsymbol{\tau}) = 0 \tag{2}$$

$$\frac{\partial E}{\partial t} + \nabla.[(E+P)\boldsymbol{u} - \boldsymbol{\tau}.\boldsymbol{u} + \boldsymbol{q}] = 0 \tag{3}$$

$$\frac{\partial (\rho Y_s)}{\partial t} + \nabla.(\rho Y_s \boldsymbol{u} - \rho D_s \nabla Y_s) = \dot{\omega}_s \tag{4}$$

$$P = \rho R \sum_{s=1}^{N} \frac{Y_s}{M_s} T \tag{5}$$

where ρ is the density, $\boldsymbol{u}$ is the velocity vector, P is the pressure, δ is a unit tensor, $\boldsymbol{\tau}$ is the viscous stress tensor, E is the total energy $\left(E = \rho e + \frac{1}{2}\boldsymbol{u}.\boldsymbol{u}\right)$, $\boldsymbol{q}$ is the heat flux vector, e is the internal energy, Y_s is the mass fraction, D_s is the diffusion coefficient, $\dot{\omega}_s$ is the production rate of each species s, R is the universal gas constant (R= 8.314 $\mathrm{Jmol^{-1}K^{-1}}$), T is the temperature, and M_s is the molar mass of each species. Here the subscript $s = 1 \sim N$ where N is the total number of species.
The viscous stress tensor $\boldsymbol{\tau}$ is defined by

$$\boldsymbol{\tau} = \mu(2\boldsymbol{S}) - \frac{2}{3}\mu(\nabla.\boldsymbol{u})\delta \tag{6}$$

where μ is the viscosity of the mixtures and $\boldsymbol{S}$ is the symmetric strain rate tensor. The heat flux vector $\boldsymbol{q}$ is defined as

$$\boldsymbol{q} = -K\nabla T - \rho\sum_{s=1}^{N} h_s D_s \nabla Y_s \tag{7}$$

where K is the thermal conductivity of the mixtures and h_s is the enthalpy of each species. The detailed computational procedure and mathematical model have been described by Terashima and Koshi [13].

3. Computational Model and Condition

In this study, knocking combustion is modeled using a one-dimensional reactor, as shown in Fig. 1. Such a model has been used in several previous studies [8,11,12]. The length of the reactor is $L = 4.0$ cm. In the left boundary, the symmetric condition is used and the adiabatic wall condition is assumed at the right boundary. The initial pressure is fixed to $P_0 = 5$ atm in all conditions. To investigate the effects of knocking occurrence, Initial temperature parametrically changes from 600 to 900K (maximum of 6 cases). Premixed gas *n*-heptane/air mixtures are considered as the working fluids in this study. The equivalence ratio of the fuel is considered to parametrically change from 0.8 to 1.4 to investigate the effect of knocking occurrence. At the left boundary, a flat hot kernel of 1400K and 5 atm with a length of $L/40$ cm is initially inserted. The flame, initiated in this high-temperature spot region, propagates into left to right side in the volume reactor and establishes an end-gas region. The flame front propagation elevates the pressure and temperature in the constant volume reactor, and autoignition occurs in the unburnt end-gas region between the flame front and the wall, followed by the generation and propagation of pressure waves.

The detailed chemical kinetic reaction mechanisms are generated by KUCRS [14]; *n*-heptane consists of 373 species and 1071 reactions, which are directly used in this simulation with the help of the highly efficient numerical methodology of fast explicit time integration and the species bundling techniques. The detailed numerical methodology of chemical kinetics and species bundling techniques have been described by Terashima and Koshi [13]. A uniform grid with a minimum spacing of about 22.1 μm (1811 grid points for $L = 4.0$ cm) is used to resolve the flow fields. We used CHEMKIN-II [15,16]

libraries to calculate the ignition delay time and heat release rate of *n*-heptane/air against equivalence ratio at different initial temperature.

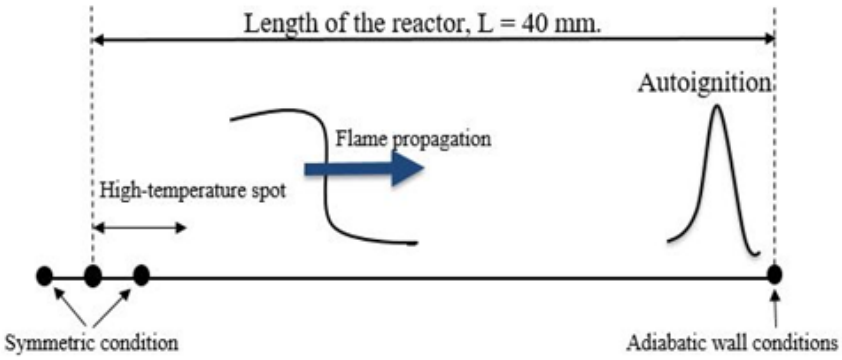

Fig. 1. Schematic of a one-dimensional reactor [13].

4. Results and Discussion

4.1. *Ignition delay time and heat release calculation*

In this study, the ignition delay time is used for validation of reaction mechanism of *n*-heptane/air. The present computation is performed under considering constant-volume adiabatic conditions and the ignition delay time is determined at the moment when the temperature exceeds 1500K. These mechanisms are generated by KUCRS [14]. To understand the effect of equivalence ratio in the 1-D knocking combustion model, the impact of ignition delay time for validation of reaction mechanisms is also considered.

Fig. 2 shows the ignition delay time of *n*-heptane/air against equivalence ratio at different initial temperatures. It is revealed that the ignition delay time decreases with the increase of equivalence ratio at different initial temperatures, which represents that the equivalence ratio influences the knocking phenomena. It also seems that with the increasing equivalence ratio, the gradual decreasing rate of the ignition delay time of n-heptane is inversely proportional. In the case of temperature, there is also a variation of ignition delay time on different initial temperature. It is exposed that the ignition delay time is more shortened at initial temperature 650K and 700K rather than 600K with increasing equivalence ratio. It can also be observed that the longer ignition delay time at 750K than at 700K at each equivalence ratio.

Heat release rate is also an important component to understand the knocking combustion. Fig. 3 represents the heat release rate of *n*-heptane for different initial temperatures with the increasing equivalence ratio. It is observed that heat release changes proportionally with the increase of initial temperature and it is also varying with increasing equivalence ratio. At initial temperature 600K, a small heat release occurs due to slow chemical reactions for different equivalence ratios. However, when the initial

temperature increases to 700K or more than 700K, a chemical reaction starts a little early compared to the lower initial temperature and higher heat release occurs due to this early chemical reaction. With the increase of equivalence ratio, heat release rate becomes growing up to a certain stage, and maximum heat release rate occurs at equivalence ratio 1.2 rather than 1.4.

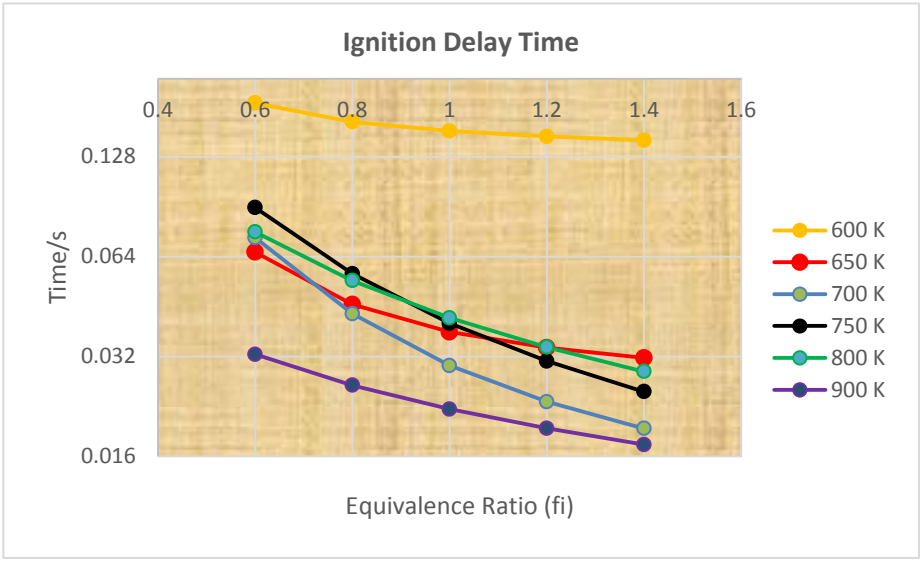

Fig. 2. The ignition delay time of *n*-heptane/air under constant volume adiabatic condition.

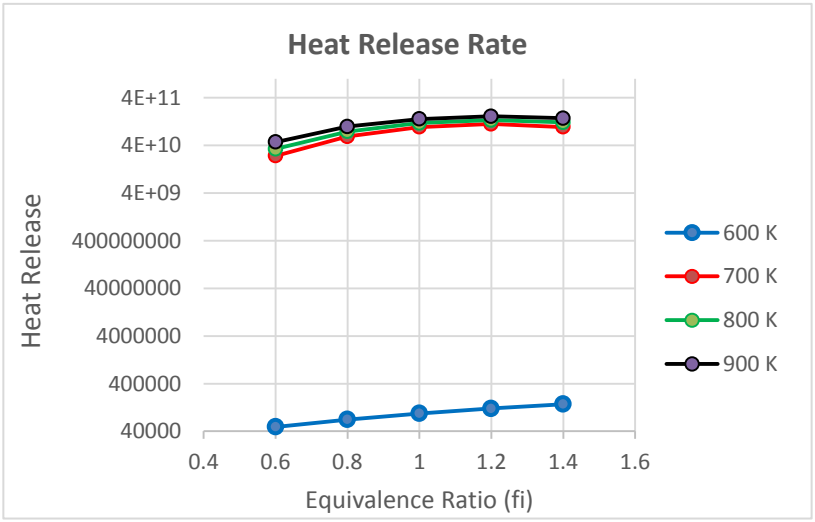

Fig. 3. Heat release rate of n-heptane in different under constant volume adiabatic condition.

4.2. *Effect of equivalence ratio on knocking occurrence at different initial temperature*

The time histories of pressure and temperature at the wall ($x = 4.0$ cm) for *n*-heptane /air mixtures have been shown in Figs. 4-5, which represent the effects of equivalence ratio on knocking occurrence at initial temperature 600K and 650K, respectively. Due to the adiabatic compression caused by the flame propagation, the pressure and temperature in the reactor gradually increase with time for each case. When the end-gas autoignition occurs before the flame front reaches the wall, then the pressure and temperature in the end gas region rapidly increase and pressure waves with non-negligible amplitudes are generated, which leads to transient oscillatory profiles at the wall.

Fig. 4 exhibits the effects of equivalence ratio on knocking occurrence at initial temperature 600K. In the ignition delay time figure (Fig. 2), we obtained the longest ignition delay time at initial temperature 600K other than all other initial temperatures accounted in this study. At an equivalence ratio, $\emptyset = 0.6$, autoignition occurs lately due to long ignition delay time and a transient pressure and temperature oscillation have occurred lately due to autoignition in the end-gas portion. For all the other equivalence ratios, the autoignition occurs early than $\emptyset = 0.6$ and generates transient oscillatory profiles.

In Fig. 5, it is observed that in 650K, autoignition occurs as early as 600K due to the short ignition delay time of *n*-heptane (Fig. 2), which causes pressure and temperature oscillation early and knocking occurrence in the end-gas at each equivalence ratio. The timing of unstable pressure and temperature undulation is almost similar at the equivalence ratio 1.2 and 1.4 and creates a vibration profile.

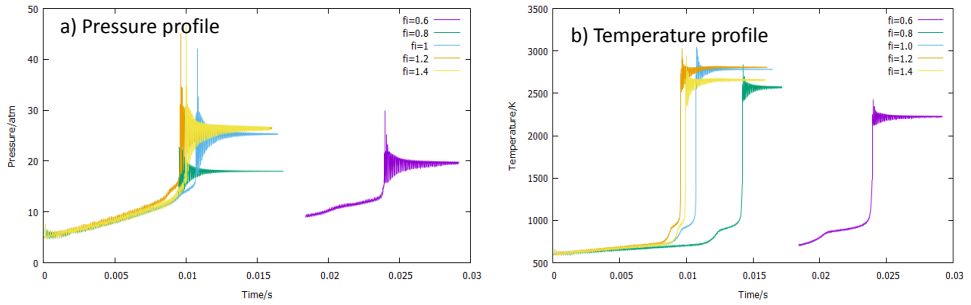

Fig. 4. Effects of equivalence ratio on transient histories at the wall ($x = 4.0$ cm) for initial temperature 600K.

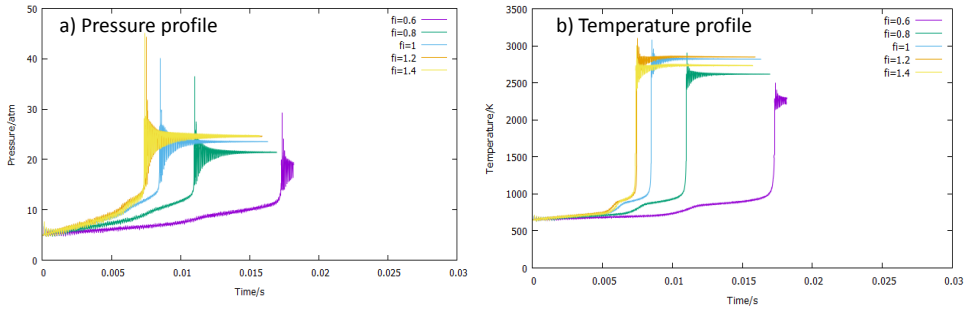

Fig. 5. Effects of equivalence ratio on transient histories at the wall ($x = 4.0$ cm) for initial temperature 650K.

Similarly, we have obtained the timing of autoignition and pressure & temperature oscillations which causes knocking occurrence with the increase of equivalence ratio at initial temperature 700, 750, 800 and 900K respectively. Fig. 6 represents the timing of autoignition, pressure & temperature oscillations against equivalence ratio at different initial temperature. It can be noted that the increasing the equivalence ratio and the initial temperature, the earlier the timing of autoignition, pressure and temperature oscillation which is the main cause of knocking occurrence. It is also observed that the timing of end-gas autoignition, pressure and temperature oscillation is very closely at the initial temperature (700–800K) and equivalence ratio (0.8–1.4).

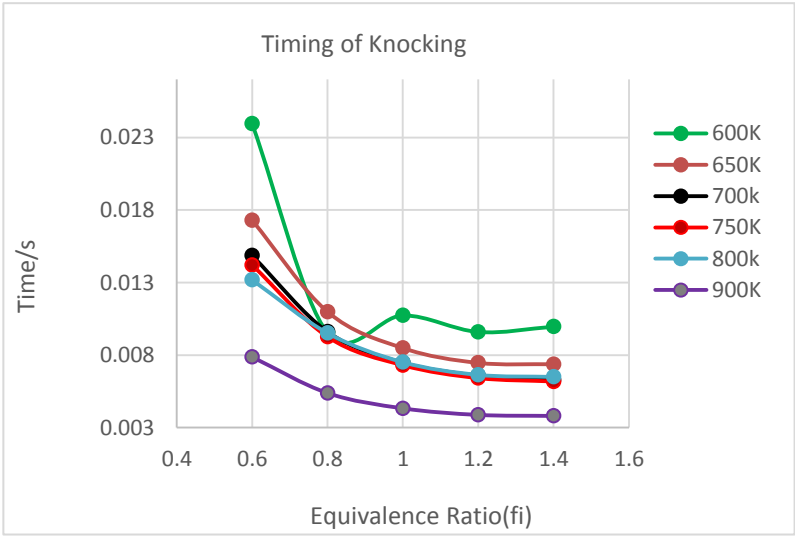

Fig. 6. Effects of equivalence ratio on timing of autoignition and pressure and temperature oscillation of *n*-heptane at different initial temperature.

4.3. *Knocking intensity*

The consequence of the last section exhibits that end-gas autoignition produces the pendulous profiles of pressure and temperature. Now we concentrate on the propagation of pressure oscillation, i.e., how pressure wave with massive amplitudes is created. To measure the excellence of pressure vibration we need to know the knocking intensity. The knocking intensity is defined as

$$\bar{P}_{KI} = \frac{P_{max}}{P_e} \tag{8}$$

where, P_e is the equilibrium pressure ascertained from the time history of the maximum pressure and $P_{\max}$ is the first peak of the largest pressure history as displayed in Fig. 7. Note that the second and third apex of the maximum pressure history may be larger than the first peak $P_{\max}$ cause of wave interactions at the symmetric or wall boundary, which is not taken into account in this study.

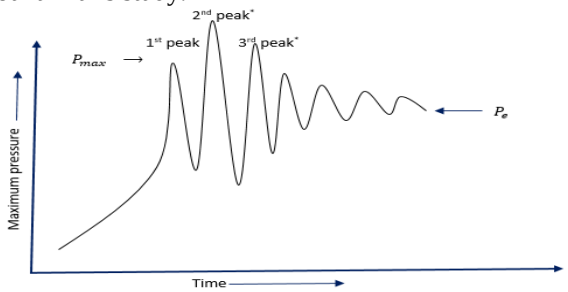

Fig. 7. Schematic of the time history of the maximum pressure for the knocking intensity with P_{max} and P_e indicated (*2nd and 3rd peaks from wave interactions at wall and symmetric conditions) [13].

Fig. 8 shows the result of the knocking intensity estimated by equation (8) against initial temperature for the case of *n*-heptane. In this Figure, we observe that for equivalence ratio 0.6, the knocking intensity constantly changes in temperatures between 600–900K with an average value of $P_{KI} = 1.24$, which shows the weak dependency of the knocking intensity of the initial temperature. For equivalence ratio 0.8, a medium peak of knocking intensity produced in 650K with a value of $P_{KI} = 2$ and on initial temperature 750–900K we see knocking intensity moderately changes with a value of $P_{KI} = 1.4$, exhibits a weak dependence of knocking. For equivalence ratio 1.0, result of the diagram exhibits a strong knocking intensity with a value of $P_{KI} = 2.4$ at an initial temperature 650K. In case of equivalence ratio 1.2 and 1.4, we find a strong knocking intensity around 600 to 700K and small knocking dependency between 750 to 800K. In increasing equivalence ratio, it is observed that the knocking intensity continuously rises at an initial temperature between 600 to 700K. At initial temperature 750K, the knocking intensity coincides each other for equivalence ratios 1.0, 1.2 and 1.4 which may be due to small pressure and temperature oscillation.

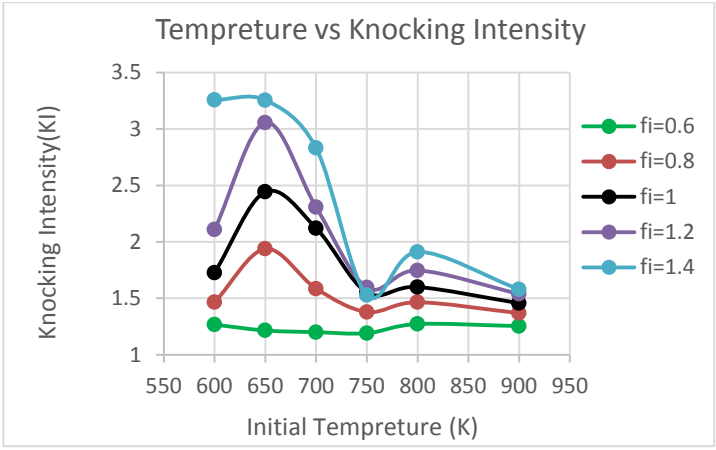

Fig. 8. Knocking intensity $\bar{P}_{KI}$ against initial temperature.

Fig. 9 exhibits the outcome of the knocking intensity calculated by equation (8) against equivalence ratio for the case of *n*-heptane. In this diagram, we obtained a strong peak of knocking intensity at around 650K at all equivalence ratios and knocking intensity continuously rises with increasing equivalence ratio where maximum knocking intensity occurred in equivalence ratio 1.4 with a value of $P_{KI} = 3.27$ approximately. On the other hand, in 750K and 900K we see that the changes of knocking intensity are continuously average in the range 1.2–1.5 with the changing of the equivalence ratio, which represents the week dependency of knocking.

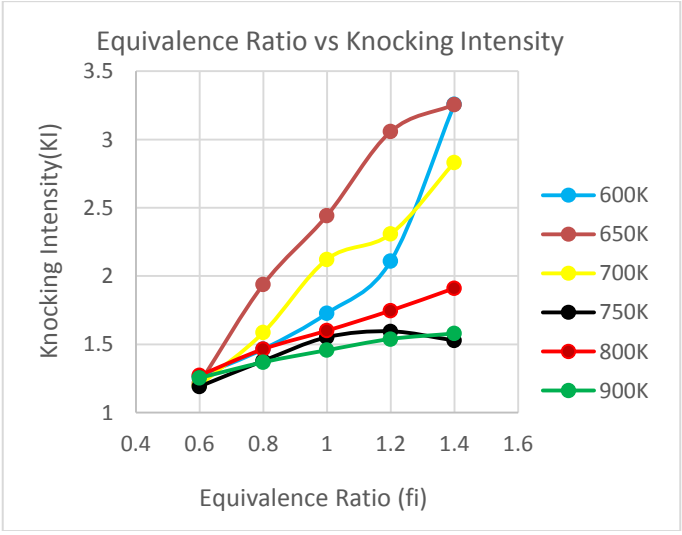

Fig. 9. Knocking intensity $\bar{P}_{KI}$ against equivalence ratio.

4.4. *Strong knocking intensity in around 650K*

In the previous section, we discussed the knocking intensity of *n*-heptane/air case in each equivalence ratio on account of initial temperature. We ascertained that in initial temperature 650K, there is a significant peak of knocking intensity produced in each equivalence ratio except 0.6. Detailed behaviors of pressure and temperature waves during end-gas autoignition are investigated to identify the origin of large knocking intensity of the *n*-heptane. In the reactor, end-gas autoignition starts at a small region adjacent to the walls, generating distinct pressure and temperature waves that propagate towards the left boundary. Due to end-gas autoignition, the flame front gradually moves back, i.e., the expansion of the end-gas, which interacts with the temperature wave in the middle of the reactor. After the interaction, the pressure and temperature waves continue to propagate in the reactor, which is the main cause of the generation of transient oscillatory pressure and temperature profiles.

Fig. 10(a-b) describes a temporal sequence of pressure and temperature profiles, respectively, with number labeling each profile of equivalence ratio 0.6 at initial temperature 650K. It is seen in Figs. 10(a) and 10(b), autoignition takes place near the wall (profiles 1-3) and creates very small pressure and temperature oscillations probably due to small heat release rate. Pressure and temperature gradually rise in the end gas (profiles 4-8), which creates a small vibration in the reactor. In this case, a strong pressure wave is not developed in the end gas region, which indicates a weak knocking intensity for an equivalence ratio 0.6.

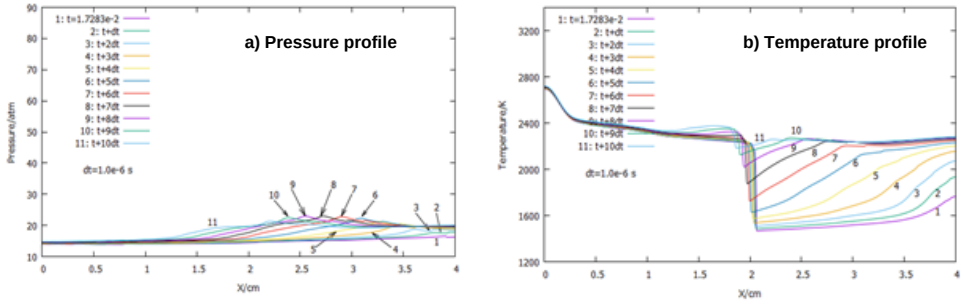

Fig. 10. A temporal sequence of pressure and temperature profiles for equivalence ratio fi=0.6 at initial temperature 650K.

On the other hand, Fig. 11(a-b) exhibits a sequence of pressure and temperature profiles with number labeling each profile of equivalence ratio 1.4, which demonstrates that the largest knocking intensity has been attributed in 650K. It is observed that clearly in Fig. 11(b) that, in the end-gas, autoignition takes place in a region near the wall quickly which creates an inhomogeneity of temperature distribution. A temperature gradient is thus formed near the wall (profile 1). The temperature adjacent to the wall then rapidly increases and strong pressure and temperature waves are created (profile 2). The produced

transient pressure wave propagates to the left in the unburnt end-gas region due to the maximum heat release of the chemical reaction. The peak pressure value thus rises, reaching a maximum at 7.3695 ms (profile 6). After that, the peak pressure decreases because autoignition also occurs in the end-gas region ahead of the pressure wave and interacts with burnt gas (profiles 7-11). Due to these phenomena, a strong and the largest knocking intensity found at 650K for equivalence ratio 1.4 and this propagation mode may be termed as a developing detonation, which may lead to a detonation.

4.5. *Weak knocking intensity in around 750K*

In Figs. 8 and 9, it is acknowledged that a weak knocking intensity has been found for *n*-heptane/air case at an initial temperature in around 750K for each case of equivalence ratio. A strong pressure wave is not so developed in 750K which causes weak-sensitivity of knocking. In this section, we have discussed the temporal sequence of pressure and temperature profile of initial temperature 750K for equivalence ratio 0.6 and 1.4.

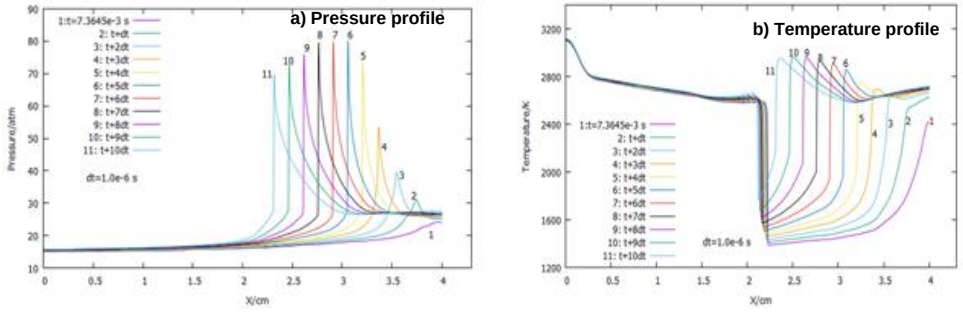

Fig. 11. A temporal sequence of pressure and temperature profiles for equivalence ratio fi=1.4 at initial temperature 650K.

A temporal sequence of pressure and temperature profiles with number labeling each profile of equivalence ratio 0.6 have been demonstrated in Fig. 12(a-b), respectively, at initial temperature 750K. In Fig. 12(a-b) it is observed that due to the slow chemical reaction a small heat release occurs in the end-gas region. Pressure and temperature gradually increase with no appearance of a small hot-spot (profile 1-3). In this reason, a pressure wave is not developed in the end-gas and pressure, and the temperature slowly increases in the end-gas region (profile 4-9) which indicates a weak intensity of knocking for equivalence ratio 0.6.

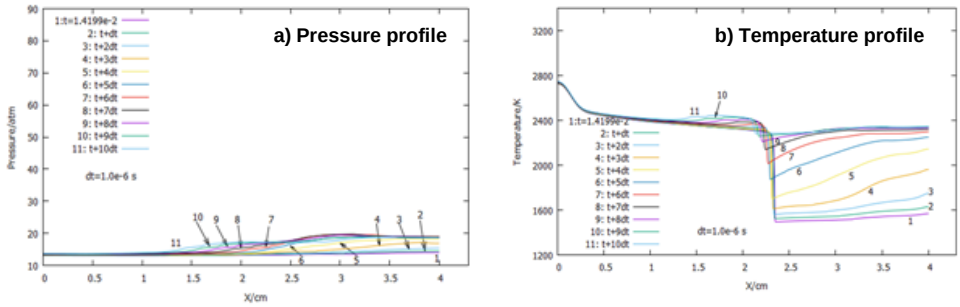

Fig. 12. A temporal sequence of pressure and temperature profiles for equivalence ratio fi=0.6 at initial temperature 750K.

On the other hand, at equivalence ratio 1.4, From the Fig. 13(a-b) it is also observed that autoignition takes place in the end-gas near the wall (profile 1-3) and due to autoignition, pressure, and temperature uniformly increases in the end-gas region (profiles 4-6). Increased pressure and temperature generates a small and transient pressure and temperature wave which propagates to the left in the unburnt gas region (profiles 7-11). This propagation mode is also known as a rapid autoignition deflagration mode, but it's not a developing detonation [8]. Due to this propagation mode, a strong pressure wave is not generated in the end gas which demonstrates a weak knocking intensity at initial temperature 750K for equivalence ratio 1.4.

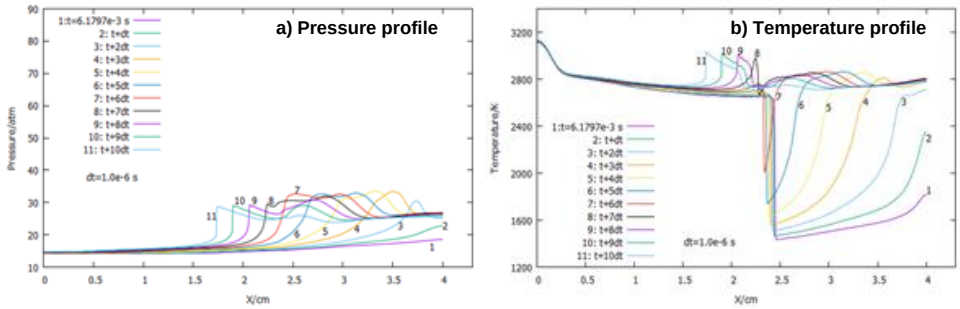

Fig. 13. A temporal sequence of pressure and temperature profiles for equivalence ratio fi=1.4 at initial temperature 750K.

5. Conclusion

In this present study, a detailed numerical simulation under constant volume adiabatic condition has accomplished for a knocking combustion model using a one-dimensional constant volume reactor. Detailed mechanisms of pressure wave generation in the end-gas autoignition at different initial temperature for various equivalence ratios have been discussed together. In this study, premixed gas *n*-heptane/air is considered with detailed chemical kinetics mechanism, which is directly introduced as a compressible fluid.

In the present study, we considered the equivalence ratios 0.6–1.4 and initial temperatures 600–900K to identify the knocking behaviors and to investigate the mechanism of pressure wave generation during knocking combustion under the condition of an adiabatic wall. The major outcomes obtained in this numerical study are summarized as follows:

- On the basis of the present equivalence ratios, the largest knocking intensity occurs at equivalence ratio 1.4 due to maximum heat releases; the smallest knocking intensity occurs at equivalence ratio 0.6 probably due to the small heat release rate.
- In the case of temperature, a strong pressure wave is generated in the end gas region at initial temperature 650K for all equivalence ratios except an equivalence ratio 0.6 which causes the highest peak of the knocking intensity.
- A weak sensitivity of knocking intensity found at an initial temperature in around 750K for all equivalence ratios.
- According to the heat release of the sequential profile of pressure, we obtained a weak-knocking intensity when equivalence ratios are smaller.

Acknowledgment

The first author is grateful to the Hokkaido University, Japan for accepting him as M.S. internship student and funding during his stay in Japan. He would like to offer his especial thanks to Professor N. Oshima for his guidance and support throughout this research work at Hokkaido University. He would also like to acknowledge the "National Science and Technology Fellowship" under the Ministry of Science and Technology for partial support of this research work.

References

1. J. B. Heywood, Internal Combustion Engine Fundamentals (McGraw-Hill, New York, 1988).
2. Z. Wang, H. Liu, and R. D. Reitz, Prog. Energy Combust. Sci. **61**, 78 (2017). https://dx.doi.org/10.1016/j.pecs.2017.03.004.
3. X. Zhen, Y. Wang, S. Xu, Y. Zhu, C. Tao, T. Xu, and M. Song, Appl. Energy **92**, 628 (2012). https://doi.org/10.1016/j.apenergy.2011.11.079.
4. N. Kawahara and E. Tomita, Int. J. Hydro. Energy **34(7)**, 3156 (2009). https://doi.org/10.1016/j.ijhydene.2009.01.091.
5. M. Pöschl and T. Sattelmayer, Combust. Flame **153(4)**, 562 (2008). https://doi.org/10.1016/j.combustflame.2007.11.009.
6. T. Lu and C. K. Law, Prog. Energy Combust. Sci. **35(2)**, 192 (2009). https://doi.org/10.1016/j.pecs.2008.10.002.
7. W. J. Pitz and C. K. Westbrook, In: Dynamics of Reactive Systems Part II: Modelling and Heterogeneous Combustion, Progress in Astronautics and Aeronautics Series (American Institute of Aeronautics and Astronautics, 1986) **105**, pp. 115-130.
8. X. Gu, D. Emerson, and D. Bradley, Combust. Flame **133(1)**, 63 (2003). https://doi.org/10.1016/S0010-2180(02)00541-2.
9. P. Dai, Z. Chen, S. Chen, Y. Ju, and Z. Chen, Proc. Combust. Inst. **35(3)**, 3045 (2015). http://dx.doi.org/10.1016/j.proci.2014.06.102.
10. D. Bradley and G. Kalghatgi, Combust. Flame **156(12)**, 2307 (2009). https://doi.org/10.1016/j.combustflame.2009.08.003.

11. Y. Ju, W. Sun, M. P. Burke, X. Gou, and Z. Chen, Proc. Combust. Inst. **33(1)**, 1245 (2011). https://doi.org/10.1016/j.proci.2010.06.110.
12. J. B. Martz, G. A. Lavoie, H. G. Im, R. J. Middleton, A. Babajimopoulos, and D. N. Assanis, Combust. Flame **159(6)**, 2077 (2012). https://doi.org/10.1016/j.combustflame.2012.01.011.
13. H. Terashima and M. Koshi, Combust. Flame **162**, 1944 (2015). https://doi.org/10.1016/j.combustflame.2014.12.013.
14. A. Miyoshi, KUCRS software library <http://www.frad.t.u-tokyo.ac.jp/~miyoshi/KUCRS/> for update information. The program uses THERM program for thermodata generation.
15. R. Kee, F. Ruply, and J. Miller, Chemkin-II: A Fortran Chemical Kinetics Package for the Analysis of Gas-Phase Chemical Kinetics, Sandia Report SAND89-8009, 1989.
16. R. Kee, G. Dixon-Lewis, J. Warnatz, M. Coltrin, and J. Miller, A Fortran Computer Code Package for the Evaluation of Gas-Phase, Multicomponent Transport Properties, SAND86-8246, 1986.